

Cherenkov Telescope results on gamma-ray binaries

Juan Cortina

Abstract In the past ten years of regular operations, a new generation of Cherenkov telescopes have established binary systems as a new class of Very High Energy γ -ray (VHE) emitters. Particle acceleration in these systems may occur either in an accretion-powered jet (“microquasar”) or in the shock between a pulsar wind and a stellar wind (“wind-wind”). This paper describes the phenomenology of the three VHE binaries PSR B1259-63, LS 5039 and LS I +61 303. Two other objects may belong to this new class: HESS J0632+057 is a point-like variable VHE source whose multiwavelength behaviour resembles that of the other binaries, whereas Cyg X-1 is a well-known accreting system which may have been detected in VHE during a flaring episode. The paper concludes with a review of the latest searches for other binaries with Cherenkov telescopes, with special emphasis on Cyg X-3.

1 Introduction

The VHE (or TeV) band covers photon energies in excess of a few tens of GeV and it is mainly studied with ground-based Imaging Atmospheric Cherenkov Telescopes (IACTs). Results presented here mostly refer to the latest generation instruments H.E.S.S., MAGIC and VERITAS. A recent review of this young field of astronomy can be found here[1]. High Energy γ -ray (HE) detectors on board satellites such as CGRO/EGRET, *AGILE* and *Fermi*/LAT are sensitive to photon energies from tens to MeV up to tens of GeV and are reviewed elsewhere in this conference[2].

We will not dwell in this paper on the physics interpretation of the observational results, but refer the reader to other contributions to this conference[3, 4, 5, 6, 7, 8] and references within. Let us shortly mention however that theoretical models fall into two possible scenarios for the production of VHE γ -rays in binary systems. In

Juan Cortina

Institut de Física d'Altes Energies (IFAE), Edifici CN, Campus UAB, Cerdanyola del Valles, E-08193, Spain, e-mail: cortina@ifae.es

the “microquasar” scenario, particle acceleration takes place at a jet which originates at an accretion disk. This scaled-down version of an active galactic nucleus may provide significant insights into the mechanism of jet production and particle acceleration since all processes take place at significantly shorter time scales. In the “wind-wind” scenario, particle acceleration happens at the interaction region between a pulsar wind and the wind of the companion star.

We will start by describing the VHE results on the three well established γ -ray binaries PSR B1259-63, LS 5039, LS I +61 303. The compact object in the first system is a pulsar and the VHE emission can be well understood within the wind-wind scenario. The physical interpretation for the other two systems is still controversial. We will then deal with the X-ray binary Cyg X-1, for which the only evidence for VHE emission comes from a short flare marginally detected by MAGIC, and with another object, HESS J0632+057, which is an established source of VHE emission, but whose association to a binary system is still uncertain. We will close the paper with a review of several X-ray binaries which have been actively searched for at VHE energies, but which remain undetected.

2 Detected in VHE: PSR B1259-63, LS 5039 and LS I +61 303

2.1 PSR B1259-63/LS 2883

PSR B1259-63/LS 2883 was the first binary established at VHE. It was discovered using the H.E.S.S. telescope array in 2004[9].

The binary system is formed by a 48 ms pulsar and a B2Ve star at a distance of 1.5 kpc (for a summary of the system parameters, see [10]). There is no evidence for jets and the compact object is a pulsar, so particle acceleration probably takes place at a shock between the pulsar wind and the wind of the stellar companion. In fact VHE emission through Inverse Compton of shock-accelerated leptons had been predicted well before the detection[11] and PSR B1259-63/LS 2833 had already been classified as a binary system with a plerionic component in [10].

The orbit is highly eccentric ($e=0.87$) and has a period of 3.4 years. Periastron takes place at a distance of 0.7 A.U., while apastron happens at around 10 A.U. Close to periastron, the pulsar travels through the stars circumstellar disk, which is inclined $10-40^\circ$ to the orbital plane. The radio pulse vanishes from around 15 days before to around 15 days after periastron due to absorption in the disk.

The long and eccentric orbit complicates the VHE observations, as the source is only bright in VHE for a few months every 3.4 years and observational constraints further limit the coverage during this period. In fact the source could never be observed in the 2-3 days around periastron so far. The first H.E.S.S. campaign during the periastron passage in 2004 revealed a complex light curve (see black points in Fig. 1). Observations could only start when the source was already 10 days before periastron. The VHE flux was actually decreasing from a maximum of $\sim 10\%$ of the

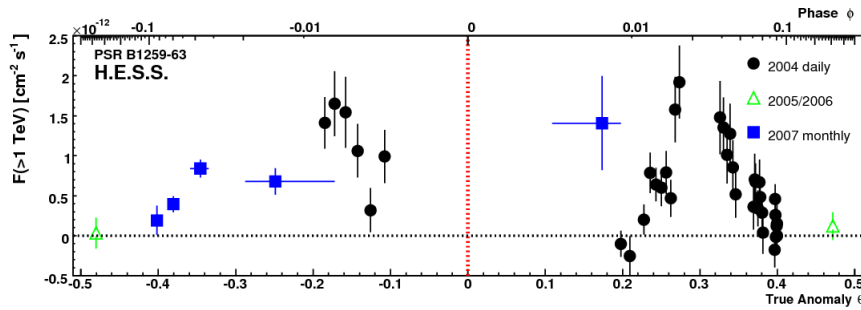


Fig. 1 VHE integrated flux from PSR B1259-63 above 1 TeV as a function of the true anomaly. The corresponding orbital phases (mean anomaly) are shown on the upper horizontal axis. The red vertical line indicates the periastron passage. Shown are data from the years 2004 to 2007: the black points are the daily fluxes as measured in 2004. The green empty triangles show the overall flux level as seen in 2005 and 2006. The blue filled squares represent the monthly fluxes taken from the campaign in 2007. From [14].

Crab Nebula flux on the first nights of observation. It followed a gap during periastron and the source was found to be brightening again up to another maximum at $\sim 10\%$ of Crab. The flux then decreased steadily for the following three months. This peculiar behaviour has been linked to the influence of the Be star disc on the emission process [12, 13].

The spectrum could be fitted to a power law with $\Gamma = 2.7 \pm 0.2$ (stat) ± 0.2 (sys) with no indication of index variability. The VHE flux corresponds to a luminosity of 8×10^{32} erg/s, which represents only 0.1% of the pulsar's spindown luminosity.

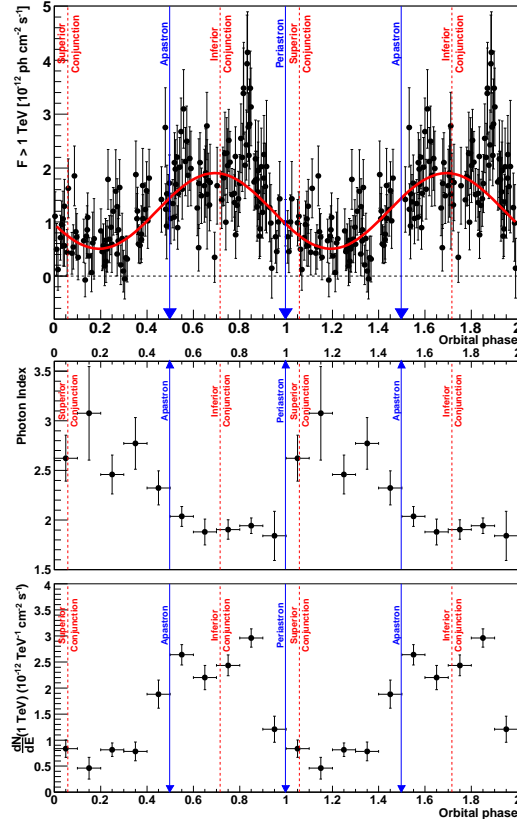
Figure 1 shows the VHE flux of the source as a function of the true anomaly for both the 2004 periastron passage and the next passage in 2007 [14]. It was again impossible to observe strictly during periastron. In general terms the source displays the same level of VHE emission, but the two light curves show different shapes, even if there are no observations at exactly the same true anomalies: the VHE seems to be brighter at $\theta = -0.3$ in 2004, but dimmer after periastron, at $\theta = +0.2$. This different behaviour in 2007 challenges models where the double-hump structure is associated to the pulsar crossing the disc.

2.2 LS 5039

This binary system consists of a compact object and an O6.5V star of $23 M_{\odot}$. It is located a distance of ~ 2.5 kpc. The orbit has a small eccentricity $e = 0.337$ with a period of 3.9061 ± 0.0001 days. The two objects are 0.1 A.U. away at periastron ($\phi = 0$) and 0.2 A.U. away at apastron. More details about the latest orbital parameters and phase definition can be found at [15]

The nature of the compact object is unknown: it may range from a $1.4 M_{\odot}$ neutron star to a $3.7 M_{\odot}$ black hole. No pulsar has been found in radio or X-ray

Fig. 2 Top: Integral γ -ray flux ($F > 1$ TeV) lightcurve (phaseogram) of LS 5039 from H.E.S.S. data (2004 to 2005) on a 28 minute run basis folded with the orbital ephemeris in [20]. The blue solid arrows correspond to periastron and apastron. The thin red dashed lines represent the superior and inferior conjunctions of the compact object. Middle: Fitted pure power-law photon index (for energies 0.2 to 5 TeV) vs. phase interval of width $\Delta\phi = 0.1$. Bottom: Power-law normalisation (at 1 TeV) vs. phase interval of width $\Delta\phi = 0.1$. From [19].



searches, although any pulsations would probably be diluted by Compton scattering for all orbital phases. As mentioned above, no pulsations are observed when the two components of the PSR B1259-63/LS 2833 system approach periastron and the two components of LS 5039 are a comparable distance for all orbital phases. VLBA shows complex extended morphology which may look at first sight like a jet, but changes orientation as the two objects progress along the orbit[17]. This argues in favor of acceleration at the region where the pulsar wind and the companion star's wind interact, rather than acceleration in a jet.

LS 5039 was discovered in VHE by H.E.S.S. [16] during their first Galactic Plane Survey. In fact it was the only point-like source found in the survey and its position was consistent with a bright unidentified EGRET source which had been proposed as a counterpart to a binary system[18]. The spectrum could be fitted to a power law with photon index 2.12 ± 0.15 and a flux of $\sim 5\%$ Crab. The VHE luminosity was similar to the X-ray luminosity.

Further H.E.S.S. observations in 2005 allowed to establish variability and periodicity consistent with the orbital period[19]. The phase-folded flux of the source is shown in figure 2 along with the evolution of the photon index with phase. The VHE

flux changes from $\sim 15\%$ Crab at inferior conjunction (when the compact object is between the companion star and the Earth) to $\sim 5\%$ Crab at superior conjunction and the spectral shape is strongly modulated along the orbit. In fact the spectrum at inferior conjunction is not a simple power law and shows a clear hardening in the region 0.3 to ~ 20 TeV.

2.3 LS I +61 303

LS I +61 303 is a binary system formed by a compact object and a B0Ve star of $12M_{\odot}$ at a distance of $2.0 \pm 0.2 \text{ kpc}$. It has an eccentricity $e=0.54$ with 26.4960 ± 0.0028 day period (from radio observations). At periastron the two system components are separated by 0.2 A.U. ($\phi = 0.275$, see [15] for the orbital elements of the system and the definition of the phase), while at apastron they are 1 A.U. apart.

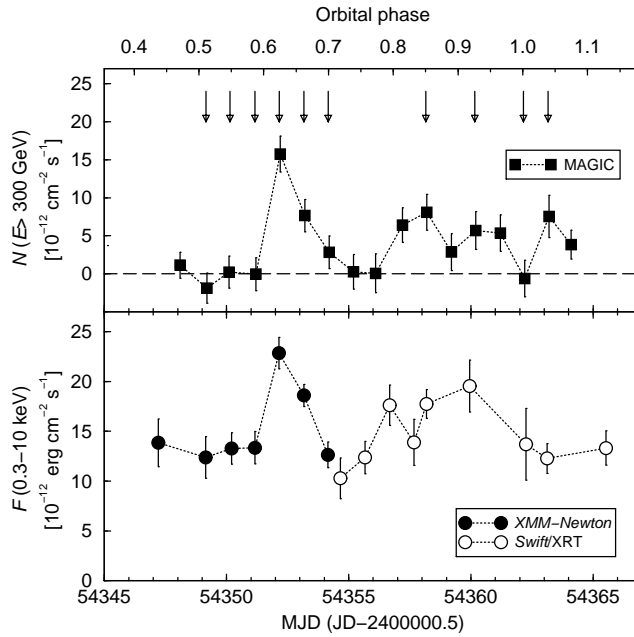


Fig. 3 VHE and X-ray light curves of LS I +61 303 during the multiwavelength campaign of 2007 September. Top: MAGIC VHE flux above 300 GeV vs. the observation time in MJD and the orbital phase. The horizontal dashed line indicates 0 flux. The vertical arrows mark the times of simultaneous VHE gamma-ray and X-ray observations. Bottom: de-absorbed flux in the 0.3–10 keV energy range for the seven XMM observations (filled circles) and the nine *Swift* ones (open circles). Error bars correspond to a 1σ confidence level in all cases. Dotted lines join consecutive data points to help following the main trends of the light curves. The sizes of the symbols are larger than the time span of individual observations. From [27].

Historically this object has drawn much interest due to its periodic outbursts in radio and X-rays. The radio outbursts are well correlated with the orbital period[29], although the phase of maximum emission moves from $\phi=0.45$ to 0.95 over a period of 1667 days. This superorbital variability is probably related to changes in the mass loss rate of the Be star and/or density of the circumstellar wind[30].

Even if extensively studied, we do not know the nature of the compact object: it could be anything from a $1.4M_{\odot}$ neutron star to a $4M_{\odot}$ black hole. No pulsar has been found in radio or X-ray searches, but the aforementioned considerations about absorption for LS 5039 apply here as well. Also similarly to LS 5039, VLBA observations reveal a complex morphology which is coupled with the orbital period[21], once again pointing to wind-wind interaction.

This binary system was discovered in VHE γ -rays by MAGIC in 2006[22] after following the source for a good fraction of the orbital phases over six orbital periods. The VHE emission was significantly variable: there was no detection at periastron or at inferior conjunction (i.e. when the compact object is between the companion star and the Earth, the phase for which LS 5039 reaches a maximum); the emission peaks at $\sim 15\%$ Crab before apastron ($\phi=0.6-0.7$). The spectrum is Crab-like, with a photon index of 2.6 ± 0.2 (stat) ± 0.2 (syst). The source was confirmed by the VERITAS telescope array during the next season [23]. The light curve and spectrum were found to be consistent with MAGIC results.

A second MAGIC campaign in 2006[24] combined with previous 2005 data allowed to establish that the VHE emission has a significant periodic component with a period of 26.8 ± 0.2 days, compatible with the orbital period and the period found in other wavelengths. Contrary to what happens in LS 5039, the phaseogram follows no simple sinusoidal shape.

MAGIC observations showed evidence for a second peak of VHE emission in December 2006 at $\phi=0.8-0.9$ but for only one orbit. No evidence was found for intranight variability in searches down to 15 min time scales, or for spectral variability, although it must be said that the spectral index could only be measured for phases $\phi=0.5-0.6$ and $\phi=0.6-0.7$ [24].

Multiwavelength observations with VERITAS, *Swift* and RXTE in 2007[26]) showed large X-ray variability with flux values typically varying between 0.5 and 3.0×10^{-11} erg cm $^{-2}$ s $^{-1}$ over a single orbital cycle, but the TeV sampling was not dense enough to detect a correlation between the two bands. MAGIC organized two multiwavelength campaigns. During the first campaign in 2006, with VLBA, MERLIN, e-EVN and Chandra[25], the gamma-ray and radio bands were found not to be correlated. The radio interferometers confirmed that the shape of the extended emission changes with the orbital period. No VHE/X-ray correlation could be established. In 2007, MAGIC followed the source along with the X-ray detectors XMM and *Swift* [27] for most of a single orbit. Around the maximum of the VHE emission ($\phi = 0.6-0.7$), the energy flux in X-rays was measured to be about two times larger than the energy flux in VHE, and, as can be seen in figure 3, both bands are significantly correlated: the correlation factor is $r = 0.81$, corresponding to a random probability $\sim 5 \times 10^{-3}$.

The phenomenology of the source in VHE has become even more complex after the latest observations of VERITAS in the 2008/09 and 2009/10 seasons[28, 31]. These are actually the only reported observations after *Fermi* started operations in 2008. LS I +61 303 has not been detected for any of the orbital phases. In fact making use of the full VERITAS array with nominal sensitivity has allowed to set stringent upper limits at the level of 2% Crab for the phase of the maximum VHE emission. The drop in VHE emission may be correlated with the super-orbital variability of 1667 days, which, as already mentioned, is probably associated to changes in the circumstellar disk and may hence have an impact on the efficiency of the particle acceleration or γ -ray absorption processes.

3 Uncertain VHE binaries: Cyg X-1 and HESS J0632+057

3.1 *Cyg X-1*

Cygnus X-1 is a High Mass X-ray Binary at 2 kpc distance. It represents the best established candidate for a stellar mass black hole, with a mass of more than $13 M_{\odot}$. Its optical companion is an O9.7 super-giant with a mass of $30 M_{\odot}$ and a strong stellar wind[32]. The orbit is low-eccentric with radius 0.2 A.U. and 5.6 days period.

The source belongs to the microquasar class because it displays a single-sided jet resolved at milli-arcsec scales with VLBA during the X-ray hard state. The jet's opening angle is less than 2° and the bulk velocity is $>0.6c$. Some authors[33] have suggested that Cygnus X-1 is a "microblazar", where the jet axis is roughly aligned with the line of sight.

1.4 GHz radio observations show a 5 pc (8 arcmin) diameter ring structure of bremsstrahlung emitting ionized gas at the shock between the jet and the interstellar medium. The power released by the (dark) jet is of the same order or the bolometric X-ray luminosity and two orders of magnitude higher than that inferred from the radio spectrum[34].

The results from observations in the soft γ -ray range with COMPTEL [35] and INTEGRAL [36] strongly suggest the presence of a non-thermal component extending beyond the hard X-ray band. In addition, fast episodes of flux variation by a factor between 3 and 30 have been detected at different time scales, ranging from milliseconds in the 3-30 keV band [37] to several hours in the 15-300 keV band [38].

MAGIC observed this microquasar for 40 h in 2006[39]. No VHE emission was found either at the microquasar or at the interaction point between the jet and the interstellar medium. Cyg X-1 however showed evidence for emission for around 1 hour in September 24th with a pre-trial significance of 4.9σ . Given the number of observed hours, this corresponds to a post-trial significance of 4.1σ . The observation stopped at sunset and could only be resumed on the following night, so the high level of VHE emission may have extended for as long as one day.

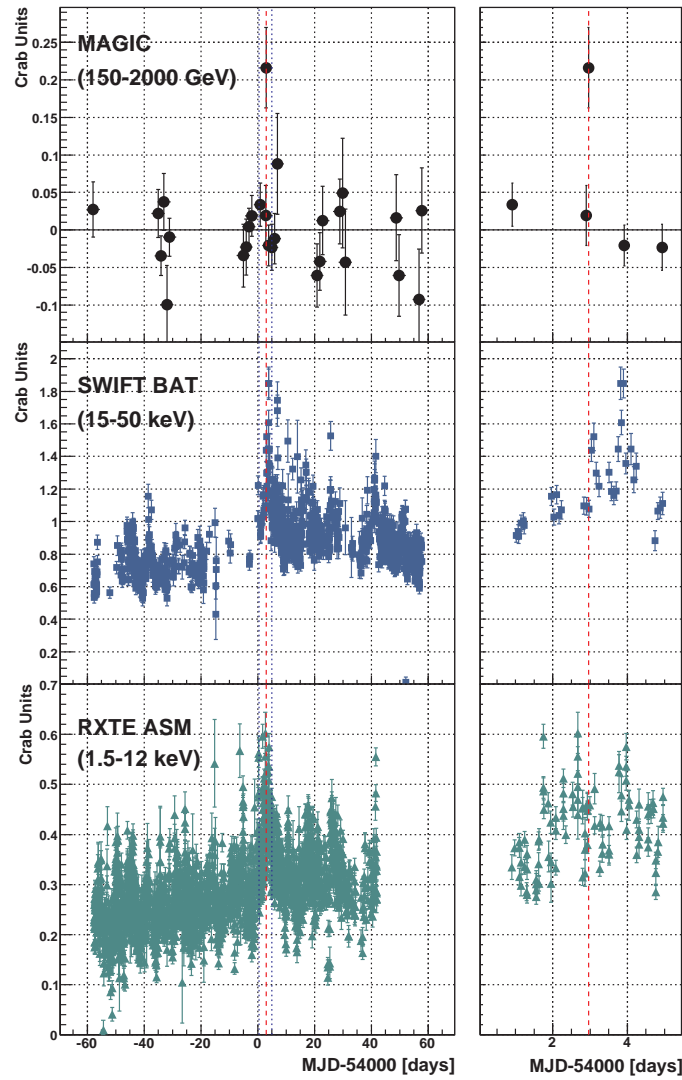


Fig. 4 From top to bottom: MAGIC, *Swift*/BAT and *RXTE*/ASM measured fluxes from Cygnus X-1 as a function of the time. The left panels show the whole time spanned by MAGIC observations. The vertical, dotted blue lines delimit the range zoomed in the right panels. The vertical red line marks the time of the MAGIC signal. From [39].

During the 79 minutes when the VHE signal was found (MJD 54002.928 and 54002.987) the VHE spectrum could be fitted to a power law with a rather soft spectral index of 3.2 ± 0.6 and a differential flux of roughly 10% Crab at 1 TeV.

Figure 4 shows the VHE, soft X-ray (RXTE/ASM) and hard X-ray (*Swift*/BAT) light curves of the source during the MAGIC observation campaign in 2006. It is especially suggestive that the VHE signal was correlated with an increase both in soft and hard X-rays, although it must be said that Cyg X-1 was in a similarly high level of X-ray emission in the following night and MAGIC did not detect it in VHE. INTEGRAL also reports a historically high flux around the same time (~ 1.5 Crab between 2040 keV and ~ 1.8 Crab between 4080 keV).

The long exposure also allowed to set stringent upper limits to the low-hard state of the binary system: any steady VHE flux due to the persistent jet associated to this X-ray state is below the present IACTs sensitivity.

For the time being, this remains the only evidence for VHE emission in an accreting binary system. Detection of such an object would allow to determine the maximum particle energy which can be achieved in the jet of a stellar-mass black hole, a fact which may help to understand the general mechanism of jet acceleration.

3.2 *HESS J0632+057*

HESS J0632+057 is one of very few point-like (< 2 arcmin) unidentified sources in the H.E.S.S. galactic plane survey [40, 41]. It was discovered using 13.5 hours of data collected between March 2004 and March 2006. The source is located in the region of the apparent interaction between the Monoceros Loop and the Rosette Nebula. Nevertheless no evidence has been found for an associated molecular cloud in NANTEN CO data. No object at the position of *HESS J0632+057* is listed in the *Fermi*/LAT first source catalogue [42, 2].

Subsequent XMM observations [43] revealed an X-ray source coincident with the massive B0pe star MWC 148 (HD 259440). However it is not known if MWC 148 is isolated or is part of a binary system. The X-ray spectrum can be fitted to an absorbed power law with $\Gamma = 1.26$ and displays significant variability on hour timescales. The spectral energy distribution (SED) of the source resembles that of LS I+61 303.

Adding to the evidence that *HESS J0632+057* is associated to a VHE binary, VERITAS observations in 2006 and 2008/09 showed no VHE emission from the source [44]. The corresponding upper limits, shown in Fig. 5 along with the fluxes measured by H.E.S.S., allow to conclude that *HESS J0632+057* is a variable VHE source with 99.993% probability.

The VERITAS campaign was simultaneous with radio and X-ray observations. VLA and GMRT radio observations [45] find a point-like (< 2 arcsec) counterpart consistent with the SED and showing variability faster than one month. X-ray observations using *Swift* [46] from MJD 54857 to 54965 also showed variability in flux (by a factor 1.8) and spectral shape (see Fig. 5). However, periodicity, which would strongly argue in favor of a binary system, could not be found on the probed timescales.

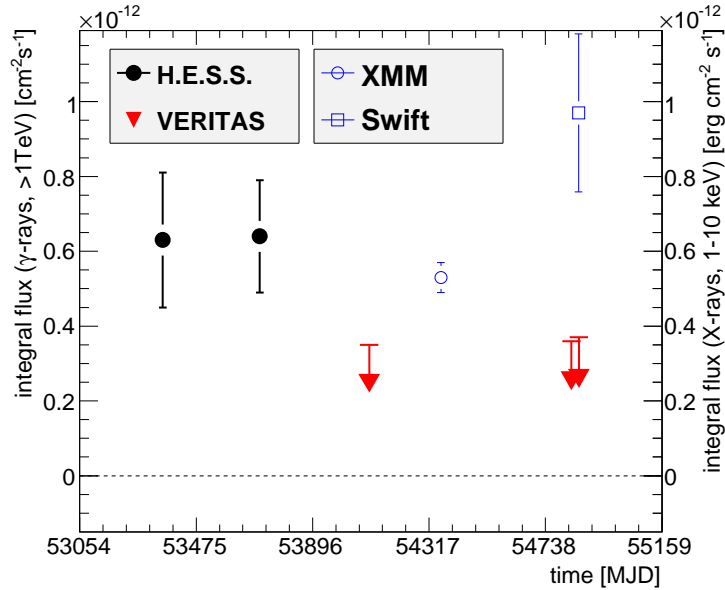


Fig. 5 Light curve above 1 TeV from HESS J0632+057 assuming a spectral shape of $dN/dE \propto E^{-\Gamma}$ with $\Gamma = 2.5$. The downwards pointing arrows show the 99% confidence limits derived from the VERITAS data. The H.E.S.S. fluxes are taken from [41]. The X-ray fluxes measured by *XMM-Newton* and *Swift* are indicated by open symbols. From [44].

4 Searches for other VHE binaries

IACTs have searched unsuccessfully for VHE emission from numerous other binary systems over the past 20 years. We will mention here a few of these results.

SS 433 is the first stellar object in which relativistic jets were discovered. It is an eclipsing binary system containing a $9 M_{\odot}$ black hole orbiting every 13.1 days a $30 M_{\odot}$ A3-7 supergiant star in a circular orbit [47, 48]. The system displays relativistic jets at a velocity of $0.26c$. The jets precesses with a period of 162.4 days. SS 433 is surrounded by the radio shell of W50, a large $2^{\circ} \times 1^{\circ}$ nebula catalogued as SNR G39.72.0. It is widely accepted that its present morphology resulted from interactions between the jets of SS 433 and the surrounding nebula. Like in Cyg X-1, the production of VHE γ rays in the SS 433/W50 system could come both from the jet inner regions or from the interaction zones where the jet impacts the surrounding nebula. SS 433 has been observed by Whipple [49], HEGRA [50], H.E.S.S. [40], MAGIC [55], VERITAS [60] and CANGAROO-II [51], but no detections have been reported either from the binary system or from the surrounding nebula.

GRS 1915+105 (or V1487 Aql) is a low mass X-ray binary consisting of a K star with a mass of less than $1.3 M_{\odot}$ on a 33 day orbit around a black hole of about

$14 M_{\odot}$ [52]. It was established as the first galactic superluminal source after the discovery of two-sided radio knots moving away from the core with true velocity greater than $0.9c$ [53]. The source was not discovered at the HEGRA or H.E.S.S. surveys of the galactic plane[54, 40]. The MAGIC telescope observed GRS 1915+105 for ~ 22 h and obtained an upper limit of 0.7% of Crab Nebula flux at the 95% confidence level[55], above 250 GeV and assuming a power law spectrum with the photon index $\Gamma=2.6$. H.E.S.S. observed the object in 2004-2008 and found no evidence for a VHE gamma-ray signal either from the direction of the microquasar or its vicinity[56]. An upper limit of $6.1 \times 10^{-13} \text{ph cm}^{-2} \text{s}^{-1}$ at the 99.9% confidence level was set on the photon flux above 410 GeV, equivalent to a VHE luminosity of $\sim 10^{34} \text{erg s}^{-1}$ for a distance of 11 kpc. For this source the upper limit to the VHE to X-ray luminosity ratio is at least four orders of magnitude lower than the ratio observed in the established VHE binaries. The VHE radiative efficiency of the compact jet is less than 0.01% based on its estimated total power of $10^{38} \text{erg s}^{-1}$.

Since VHE emission is due to particle acceleration in stellar wind/pulsar wind interaction shock in at least one VHE binary, we may also expect to detect VHE γ -rays from binaries where one of the components is a Wolf-Rayet (WR). MAGIC has observed two archetypical WR binaries[57]: WR 147 (for 30 hours in 2007) and WR 146 (for 45 hours between 2005 and 2007). No signal was found in any of the them. 95% confidence level upper limits could be set at a level of 1.5% of the Crab flux for WR 147 and 5% of the Crab flux for WR 146, both above an energy of 80 GeV. Upper limits at higher energies up to 1 TeV are even more restrictive.

Results of VHE observations of other X-ray binaries can be found in [60, 55, 58, 59]. In what remains of this section we will concern ourselves with a recent report of several years of MAGIC observations of Cyg X-3.

4.1 Cyg X-3

Cyg X-3 is a bright and persistent X-ray binary. It lies close to the Galactic plane at a distance between 3.4 and 9.8 kpc, probably at 7 kpc[61]. The nature and the mass of the compact object are still subject of debate. Published results suggest either a neutron star of $1.4 M_{\odot}$ [62] or a black hole of less than $10 M_{\odot}$ [63]. The identification of its donor star as a Wolf-Rayet star classifies it as a high-mass X-ray binary. Nevertheless Cyg X-3 shows a short orbital period of 4.8 hours, typical of low-mass binaries, which has been inferred from the modulation of both the X-ray and infrared emissions.

The source shows two main spectral X-ray states resembling the canonical states of black hole binaries: a Low/Hard (LH) and a High/Soft (HS) state [64, 66]. However the LH state displays a high-energy cut-off at ~ 20 keV, significantly lower than the ~ 100 keV value found for black hole binaries[65, 64]. Adding to its peculiarity, Cyg X-3 is the X-ray binary displaying the brightest radio emission during outbursts. It frequently exhibits huge radio flares[67] as intense as few thousand times the quiescent emission level of ~ 20 mJy at 1.5 GHz. During these outbursts, which

occur mainly when the source is in the HS state and last for several days, Cyg X-3 reveals the presence of collimated relativistic jets[68, 69, 70], a fact which grants it access to the microquasar class.

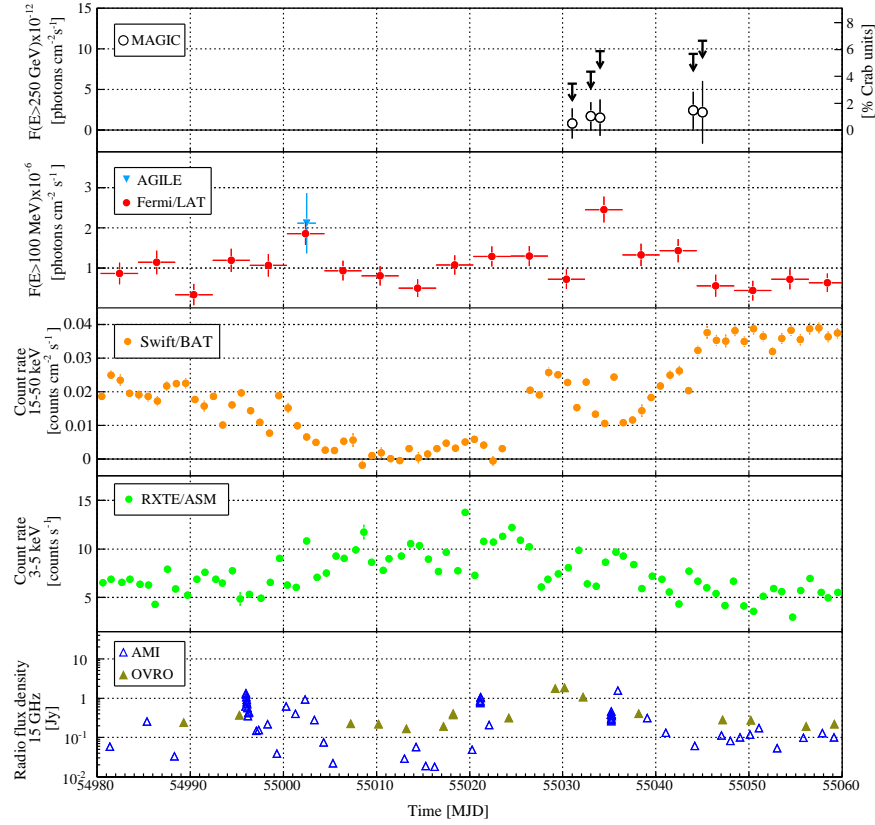


Fig. 6 From top to bottom: daily light curves of Cyg X-3 measured in VHE (MAGIC, upper limits) at energies above 250 GeV, HE γ -rays (AGILE and Fermi/LAT), hard X-rays (Swift/BAT), soft X-rays (RXTE/ASM) and radio. From [80].

Cyg X-3 has also historically drawn a great deal of attention, and in fact strongly contributed to the development of the field, due to numerous claims of detection at TeV and PeV γ -rays. However, a critical analysis of these observations raised doubts on their validity (we refer the reader to [71] and references within for all the reports of detection). In recent years, more sensitive instruments have failed to confirm those claims for energies above 500 GeV [72, 73]. Nevertheless, the fact that this object is a microquasar with the aforementioned strong X-ray and radio emission makes into a good candidate for VHE emission (see e.g. [74, 75, 76]). This radiation could have either an episodic nature due to the ejection of strong radio-

emitting blobs[77] in the HS state, or a quasi-stationary character if it is originated in the persistent compact jet present during the LH state[76].

The source has been very recently detected at high energy γ -rays by *AGILE*[78] and *Fermi*/LAT[79, 2]. *AGILE* found five γ -ray flares above 100 MeV, which were temporally correlated with transitional spectral states of the radio and X-ray emissions, whereas *Fermi*/LAT detected an orbital modulation of the flux during periods of GeV high-activity which lasted for several weeks and coincided with the source being in the HS state. *Fermi*/LAT has found the source to be variable with peaks as high as $\sim 2.0 \times 10^{-6}$ photons $\text{cm}^{-2} \text{s}^{-1}$ above 100 MeV, which are comparable and simultaneous with the *AGILE* detections. The emission during the HE active period is periodic with the orbital period of the system.

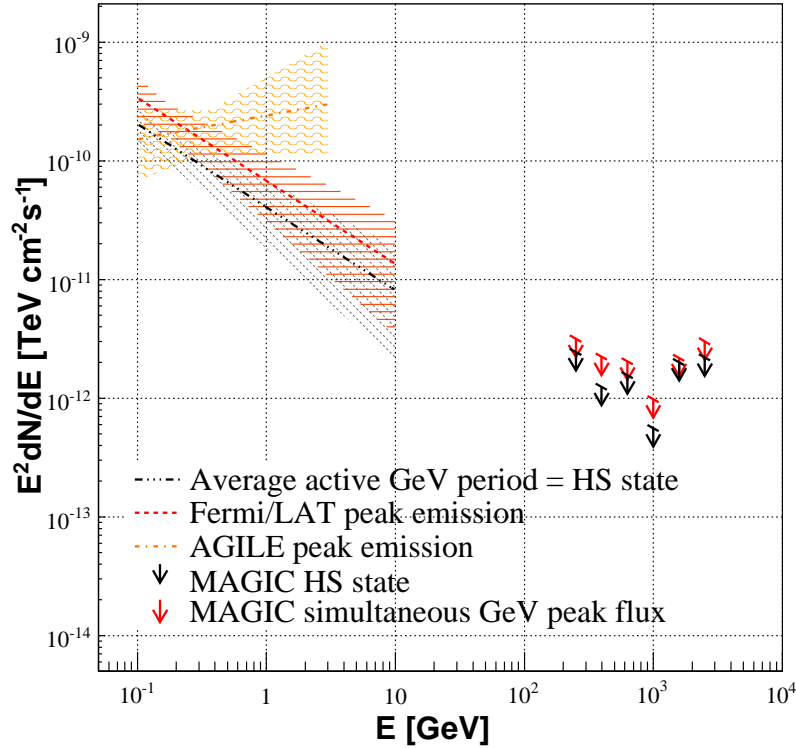


Fig. 7 Cyg X-3 spectral energy distribution in the HE and VHE bands. The lines indicate the power-law spectra derived from *Fermi*/LAT and *AGILE* integral fluxes and photon indices. The corresponding errors are shown as shadowed areas. The arrows correspond to the 95% CL MAGIC differential flux upper limits and their slope indicates the assumed power-law spectrum (photon index 2.6). The black color corresponds to the general period of *Fermi*/LAT enhanced GeV activity, which is simultaneous to the X-ray High Soft state, whereas, the red color corresponds to the highest HE peak (MJD 55031–55034). From [80].

MAGIC observed Cyg X-3[80] for about 70 hours between 2006 March and 2009 August in different X-ray/radio spectral states and also during one of the active HE periods reported by *Fermi*/LAT. No evidence was found for a VHE signal from the direction of the microquasar. An upper limit to the integral flux for energies higher than 250 GeV has been set to 2.2×10^{-12} photons $\text{cm}^{-2} \text{s}^{-1}$ (95% confidence level). It corresponds to 1.3% of the Crab Nebula flux at these energies and is most stringent limit so far to the persistent VHE emission of this source. A search for emission was performed separately for each year of observations, on a daily basis and for each orbital phase. No significant VHE emission was found in any of the three searches (for more details and differential flux upper limits, see [80]).

The VHE data sample was also split according to the X-ray state of the source. The upper limit to VHE emission during the HS state corresponds to 2.5% of the Crab Nebula flux. In the LH state, the VHE emission is expected to be produced inside the compact and persistent jets, whose total luminosity is estimated to be at least 10^{37} erg s^{-1} [81]. The MAGIC upper limit corresponds to a VHE luminosity of 7×10^{33} erg s^{-1} for a distance of 7 kpc. Thus, the maximum conversion efficiency of the jet power into VHE γ -rays is 0.07% which is similar to that of Cygnus X-1 for the upper limit on the VHE steady emission, but one order of magnitude larger than that of GRS 1915+105.

MAGIC pointed at Cyg X-3 during the second period of HE enhanced activity detected by *Fermi*/LAT in 2009, as shown in figure 6. In particular, MAGIC carried out observations simultaneous with a GeV emission peak on 2009 July 21 and 22 (MJD 55033–55034), but did not detect VHE emission. The corresponding integral flux UL above 250 GeV is lower than 6% of the Crab Nebula flux.

As can be seen in figure 7, this flux UL is roughly at the level of a power-law extrapolation of the HE flux measured by *Fermi*/LAT, assuming the photon index $\Gamma=2.6$ which *Fermi*/LAT has measured for both the low and high state of the source, but it is significantly below the extrapolation of the *Fermi*/LAT flux but assuming the photon index measured by *AGILE* only during the high state ($\Gamma=1.8$). Both results point to a cutoff in the energy spectrum of the source at energies in the range between a few GeV and 250 GeV.

5 Conclusions

VHE binaries may be powered by the interaction between a pulsar wind and the wind of its companion star, or by an accretion-driven jet.

Three binary systems have been established at the VHE band: PSR B1259-63, LS 5039 and LS I +61 303. Emission in the first binary stems from pulsar wind/stellar wind interaction, and the other two objects are consistent with the same scenario. All three sources display a complex phenomenology. Even if there is a significant component of the VHE emission which is associated to the orbital period, variations from orbit to orbit are observed. LS I +61 303 significantly dropped in brightness over the past two years and recent observations have in fact failed to detect it for

any orbital phase, a fact which may be linked to superorbital variability observed at other wavelengths.

Its variability at VHE and lower energies, its point-like character and its SED make HESS J0632+057 into a plausible candidate to become the fourth VHE binary. On the other hand, a black hole X-ray binary, Cyg X-1, has shown a marginal episodic signal at VHE, which may eventually make it into the first VHE microquasar.

Searches for other well-known X-ray binaries have proved unfruitful. Recent observations of Cyg X-3 in a wide variety of X-ray and radio states and during a high energy γ -ray flare detected by *Fermi*/LAT have not shown evidence for simultaneous VHE emission.

References

1. Hinton, J. A. and Hofmann W.: Teraelectronvolt Astronomy. *Annu. Rev. Astron. Astrophys.* **47**, 523–565 (2009).
2. Dubois, R. for the Fermi/LAT Collaboration: Fermi results on gamma-ray binaries. These proceedings.
3. Stella L.: Observational aspects of X-ray binaries. These proceedings.
4. Torres, D. F.: Gamma-ray binaries as pulsar systems. These proceedings.
5. Cerutti, : Relativistic motion and beamed radiation in gamma-ray binaries. These proceedings.
6. Moldón, J.: Astrometric and morphological variability and the birth place of LS 5039. These proceedings.
7. Zabalza, V.: Leptonic one zone model for LS I +61 303. These proceedings.
8. Casares J.: New results on VHE gamma-ray binaries. These proceedings.
9. Aharonian, F. A. et al. (the HESS coll.): Discovery of the Binary Pulsar PSRB125963 in Very-High-Energy Gamma Rays around Periastron with H.E.S.S. *A&A* **442**, 1 (2005).
10. Tavani, M. and Arons, J.: Theory of High-Energy Emission from the Pulsar/Be Star System PSR 125963. I. Radiation Mechanisms and Interaction Geometry *ApJ* **477**, 439 (1997).
11. Kirk, J. G., Ball, L., Skjaeraasen, O.: Inverse Compton emission of TeV gamma rays from PSR B1259-63. *Astrop. Phys.*, **10/1**, 31–45 (1999).
12. Kawachi, A., Naito, T., Patterson, J. R., et al.: A Search for TeV Gamma-Ray Emission from the PSR B125963/SS 2883 Binary System with the CANGAROO-II 10 Meter Telescope. *ApJ* **607**, 949 (2004).
13. Chernyakova, M., Neronov, A., Lutovinov, A., Rodriguez, J., Johnston, S.: XMM-Newton observations of PSR B1259-63 near the 2004 periastron passage. *MNRAS* **367**, 1201 (2006).
14. Aharonian, F. A. et al. (the HESS coll.): Very high energy γ -ray observations of the binary PSR B125963/SS2883 around the 2007 Periastron. *A&A* **507**, 389–396 (2009).
15. Aragona, C. et al.: The Orbits of the γ -ray Binaries LS I +61 303 and LS 5039. *ApJ* **698**, 514 (2009).
16. Aharonian, F. A. et al. (the HESS coll.): Discovery of Very High Energy Gamma Rays Associated with an X-ray Binary. *Science* **309**, 746 (2005).
17. Ribó M., Paredes J. M., Moldón J., Martí J., Massi M.: The changing millisecond radio morphology of the gamma-ray binary LS 5039. *A&A* **481**, 17–20 (2008).
18. Paredes, J. M., Martí J., Ribó M., Massi M.: Discovery of a High-Energy Gamma-Ray-Emitting Persistent Microquasar. *Science* **288**, 2340 (2000).
19. Aharonian, F. A. et al. (the HESS coll.): 3.9 day orbital modulation in the TeV gamma-ray flux and spectrum from the X-ray binary LS 5039. *A&A* **460**, 743 (2006).

20. Casares J., Ribó M., Ribas I., Paredes J.M., et al.: A possible black hole in the gamma-ray microquasar LS 5039. *MNRAS* **364**, 899 (2006).
21. Dhawan, V., Mioduszewski, A., & Rupen, M.: in *VI Microquasar Workshop: Microquasars and Beyond*, ed. by T. Belloni, (Trieste: PoS), p. 52
22. Albert, J. et al. (the MAGIC coll.): Variable Very-High-Energy Gamma-Ray Emission from the Microquasar LS I +61 303. *Science*, **312/5781**, 1771–1773 (2006).
23. Acciari, V. A. et al. (the VERITAS coll.): VERITAS Observations of the γ -Ray Binary LS I +61 303. *ApJ* **679**, 1427 (2008).
24. Albert, J. et al. (the MAGIC coll.): Periodic Very High Energy γ -Ray Emission from LS I +61 303 Observed with the MAGIC Telescope. *ApJ* **693**, 303 (2008).
25. Albert, J. et al. (the MAGIC coll.): Multiwavelength (Radio, X-Ray, and γ -Ray) Observations of the γ -Ray Binary LS I +61 303. *ApJ* **684**, 1351 (2008).
26. Acciari, V. A. et al. (the VERITAS coll.): Multiwavelength Observations of LS I +61 303 with Veritas, Swift, and RXTE. *ApJ* **700**, 1034 (2009).
27. Albert, J. et al. (the MAGIC coll.): Correlated X-Ray and Very High Energy Emission in the Gamma-Ray Binary LS I +61 303 *ApJ* **706**, 27–30 (2009).
28. Holder, J. for the VERITAS coll.: VERITAS observations of LS I +61 303 in the Fermi Era, in *31st International Cosmic Ray Conference* (Lodz, 2009).
29. Gregory, P. C.: Bayesian Analysis of Radio Observations of the Be X-Ray Binary LS I +61 303. *ApJ* **525**, 427 (2002).
30. R.K. Zamanov, R. K. et al.: Evidence of $H\alpha$ periodicities in LS I+61°303. *A&A* **351** 543–550 (1999).
31. Aliu, E. for the VERITAS coll.: Latest results on pulsar environments by VERITAS. These proceedings.
32. Ziokowski, J.: Evolutionary constraints on the masses of the components of HDE 226868/Cygnus X-1 binary system. *MNRAS* **358**, 851 (2005).
33. Romero, G. E., Kaufman Bernado, M. M., Mirabel, I. F.: Recurrent microblazar activity in Cygnus X-1? *A&A* **393**, L61–64 (2002).
34. Gallo, E., Fender, R. P., Kaiser, C., Russell, D., Morganti, R., Oosterloo, R., Heinz, S.: A dark jet dominates the power output of the stellar black hole Cygnus X-1. *Nature* **436**, 819 (2005).
35. McConnell, M. L., et al.: The Soft Gamma-Ray Spectral Variability of Cygnus X-1. *ApJ* **572**, 984 (2002).
36. Cadolle Bel, M., et al.: The broad-band spectrum of Cygnus X-1 measured by INTEGRAL. *A&A* **446**, 591 (2006).
37. Gierliński, M., Zdziarski, A. A.: Discovery of powerful millisecond flares from Cygnus X-1. *MNRAS* **343**, L84–87 (2003)
38. Golenetskii, S., Aptekar, R., Frederiks, D., Mazets, E., Palshin, V., Hurley, K., Cline, T., Stern, B.: Observations of Giant Outbursts from Cygnus X-1. *ApJ* **596**, 1113 (2003).
39. Albert, J. et al. (the MAGIC coll.): Very High Energy Gamma-ray Radiation from the Stellar-mass Black Hole Cygnus X-1. *ApJ* **665**, L51–54 (2007).
40. Aharonian, F. A. et al. (the HESS coll.): A new population of very high energy gamma-ray sources in the Milky Way. *Science* **307**, 1938 (2005).
41. Aharonian, F. A. et al. (the HESS coll.): Discovery of a point-like very-high-energy γ -ray source in Monoceros. *A&A* **469**, L1–4 (2007).
42. Abdo A. A. et al. (the Fermi/LAT coll.): Fermi Large Area Telescope First Source Catalog. *ApJ Supp. S.* **188**, 405 (2010).
43. Hinton, J. A. et al.: HESS J0632+057: A new gamma-ray binary? *ApJ Lett.* **690**, L101–104 (2009).
44. Acciari, V. A. et al. (the VERITAS coll.): Evidence for long-term gamma-ray and X-ray variability from the unidentified TeV source HESS J0632+057. *ApJ* **698**, L94–L97 (2009).
45. Skilton, J. L. et al.: The radio counterpart of the likely TeV binary HESS J0632+057 *MNRAS* **399**, 317–322 (2009).
46. Falcone, A.D. et al.: Probing the Nature of the TeV Gamma-Ray Source HESS J0632+057 with Swift. *ApJ Lett.* **708**, 52 (2010).

47. Fabrika, S. et al.: Properties of SS 433 and ultraluminous X-ray sources in external galaxies. *Astrophysics and Space Physics Reviews*, **12**, 1 (2004).
48. Cherepashchuk, A. M., et al.: INTEGRAL observations of SS433: Results of a coordinated campaign. *A&A* **437**, 561 (2005).
49. Catanese, M., Weekes, T. C.: Very High Energy Gamma-Ray Astronomy. *PASP* **111**, 1193–1222. (1999)
50. F. A. Aharonian et al. (the HEGRA coll.): TeV gamma-ray observations of SS-433 and a survey of the surrounding field with the HEGRA IACT-System. *A&A* **439**, 635 (2005).
51. Hayashi S. et al. (the CANGAROO coll.): Search for VHE gamma rays from SS433/W50 with the CANGAROO-II telescope. *Astrop. Phys.* **32**, 112–119 (2009).
52. Harlaftis, E. T., Greiner, J.: The rotational broadening and the mass of the donor star of GRS 1915+105. *A&A* **414**, L13–16 (2004).
53. Mirabel, I. F., Rodriguez, L. F.: A superluminal source in the Galaxy. *Nature* **371**, 46 (1994).
54. Aharonian, F. A. et al. (the HEGRA coll.): A search for TeV gamma-ray emission from SNRs, pulsars and unidentified GeV sources in the Galactic plane in the longitude range between -2 deg and 85 deg. *A&A* **395**, 803 (2002).
55. Saito, T. Y., Zanin, R., Bordas, P., for the MAGIC coll.: Microquasar observations with the MAGIC telescope. Proc. 31st ICRC, Lodz, Poland, July 2009, and arXiv:0907.1017.
56. F. Acero et al. (the HESS coll.): HESS upper limits on very high energy gamma-ray emission from the microquasar GRS 1915+105. *A&A* **508**, 1135–1140 (2009).
57. Aliú E. et al (the MAGIC coll.): First Bounds on the High-Energy Emission from Isolated Wolf-Rayet Binary Systems. *ApJ Lett.* **685**, L71–74 (2008).
58. Nicholas, B., Rowell, G. for the HESS coll.: H.E.S.S Observations of the Microquasars Cir X-1, Cyg X-1 and 4U 1755-33 Proc. of the 4th International Meeting on High Energy Gamma-Ray Astronomy. AIP Conference Proceedings, **1085** 245–248 (2008).
59. Chadwick P. M. for the HESS coll.: Simultaneous X-ray and VHE gamma-ray observations of microquasars. Proc. 29 Int. Cosmic Ray Conference, Pune, India, **4** 263–266 (2005).
60. Guenette R. for the VERITAS coll.: VERITAS Observations of X-ray Binaries
61. Ling, Z., Zhang, S. N., Tang, S.: Determining the Distance of Cyg X-3 with its X-Ray Dust Scattering Halo. *ApJ* **695**, 1111 (2009).
62. Stark M. J., Saia M.: Doppler Modulation of X-Ray Lines in Cygnus X-3. *ApJ Lett.* **587**, L101 (2003).
63. Hanson, M. M., Still, M. D., Fender, R. P.: Orbital Dynamics of Cygnus X-3. *ApJ* **541**, 308–311 (2000).
64. Zdziarski A. A., Gierlinski M.: Radiative Processes, Spectral States and Variability of Black-Hole Binaries. *Progr. Theor. Phys. Suppl.* **155**, 99 (2004).
65. Hjalmarsson L., et al.: INTEGRAL Observations of Cygnus X-3. Proc. of the 5th INTEGRAL Workshop “The INTEGRAL Universe”, Munich, **552**, 223 (2004), and astro-ph/0404491.
66. Hjalmarsson L., et al.: Spectral variability in Cygnus X-3. *MNRAS* **384**, 278 (2008).
67. Braes, L., Miley, G.: Radio Detection of Cygnus X-3. *Nature* **237**, 506 (1972).
68. Geldzahler, B. J., Johnston, K. J., Spencer, J. H., et al.: The 1982 September radio outburst of Cygnus X-3 - Evidence for jet-like emission expanding at not less than about 0.35c. *ApJ Lett.* **273**, L65–69 (1983).
69. Martí, J. et al., Development of a two-sided relativistic jet in Cygnus X-3, *A&A* **375**, 476 (2001).
70. Miller-Jones, J. C. A., et al.: Time-sequenced Multi-Radio Frequency Observations of Cygnus X-3 in Flare. *ApJ* **600**, 368 (2004).
71. Chardin G., Gerbier G.: Cygnus X-3 at high energies - A critical analysis of observational results. *A&A* **210**, 52 (1989).
72. Shilling, M., et al.: Recent HEGRA observations of Cygnus X-3. Proc. 27th International Cosmic Ray Conference, Hamburg, 2521–2524 (2001).
73. Albert, J., et al. (the MAGIC coll.): MAGIC Observations of the Unidentified Gamma-Ray Source TeV J2032+4130. *ApJ Lett.* **675**, L25–28 (2008).

74. Levinson, A., Blandford, R.: On the Jets Associated with Galactic Superluminal Sources. *ApJ Lett.* **456**, L29–33 (1996).
75. Romero, G. E., Torres, D. F., Kaufman Bernardo, M. M., Mirabel, I. F.: Hadronic gamma-ray emission from windy microquasars. *A&A* **410**, L1 (2003).
76. Bosch-Ramon, V., Romero, G. E., Paredes, M. J.: A broadband leptonic model for gamma-ray emitting microquasars. *A&A* **447**, 263 (2006).
77. Atayan A. M., Aharonian F. A.: Modelling of the non-thermal flares in the Galactic microquasar GRS 1915+105. *MNRAS* **302**, 253 (1999).
78. Tavani, M., et al.: Extreme particle acceleration in the microquasar CygnusX-3. *Nature* **462**, 620 (2009).
79. Abdo, A. A., et al.: Modulated High-Energy Gamma-Ray Emission from the Microquasar Cygnus X-3. *Science* **326**, 1512 (2009).
80. Aleksic, J. et al. (the MAGIC coll.): MAGIC constraints on Gamma-ray emission from Cygnus X-3. Submitted to *ApJ* and arXiv:1005.0740.
81. Martí, J., Perez-Ramírez, D., et al.: Possible hot spots excited by the relativistic jets of Cygnus X-3. *A&A* **439**, 279 (2005).